NASA
Technical
Paper
2950

November 1989

The Interlaminar Fracture Toughness of Woven Graphite/Epoxy Composites

Joan G. Funk
and Jerry W. Deaton

NASA

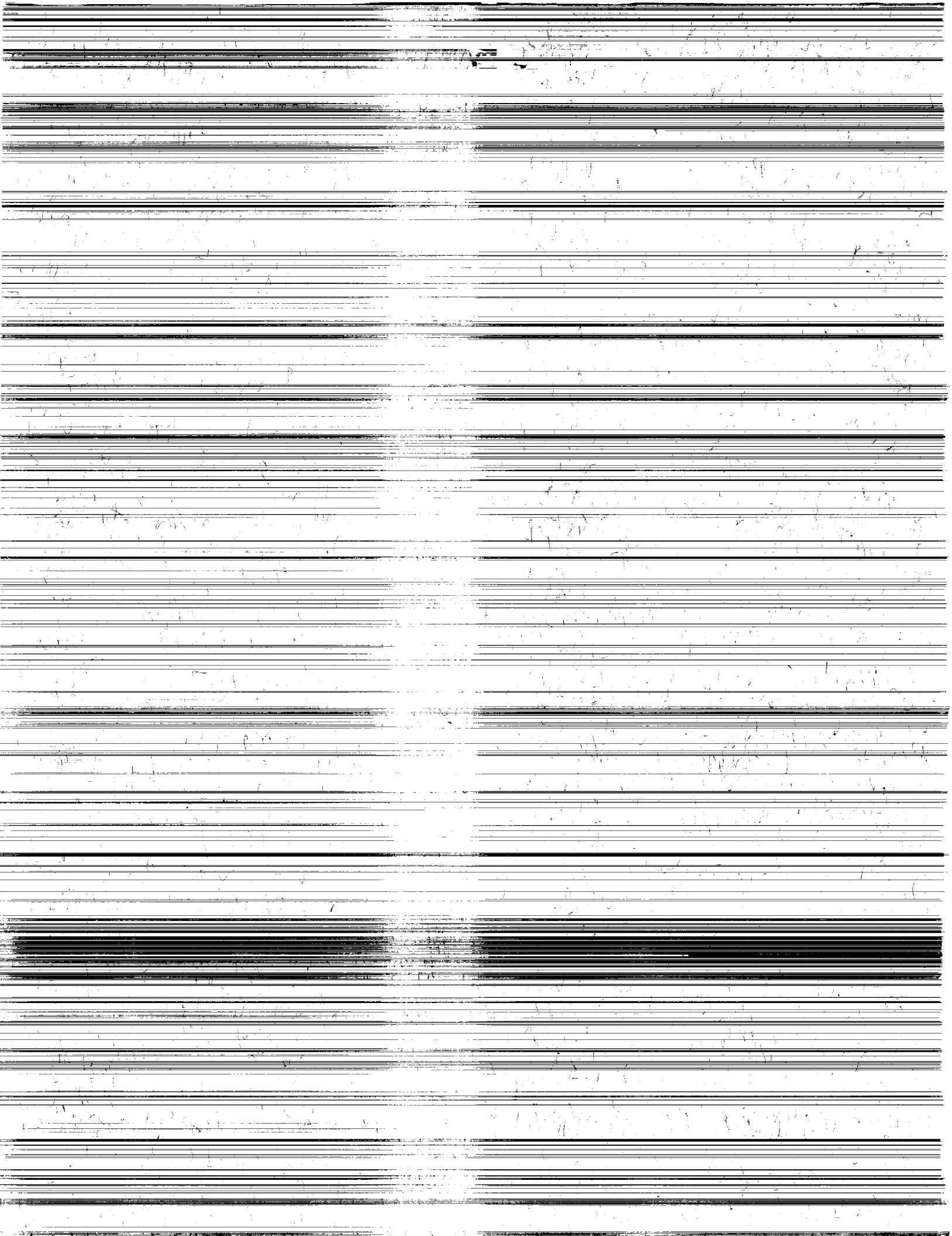

NASA Technical Paper 2950

1989

The Interlaminar Fracture Toughness of Woven Graphite/Epoxy Composites

Joan G. Funk
and Jerry W. Deaton
Langley Research Center
Hampton, Virginia

National Aeronautics and Space Administration
Office of Management
Scientific and Technical Information Division

Summary

The interlaminar fracture toughness of graphite/epoxy woven composites was determined as a function of stacking sequence, thickness, and weave pattern. Plain, oxford, 5-harness satin, and 8-harness satin weave patterns of T300/934 fabric were evaluated by the double cantilever beam test. The fabric had a mode I critical-strain-energy release rate (G_{Ic}) ranging from two to eight times greater than that of a 0° unidirectional T300/934 tape material. The interlaminar fracture toughness of a particular weave pattern was dependent on whether the stacking sequence was symmetric or asymmetric and, in some cases, on the fabric orientation.

Introduction

Low-velocity impact studies (refs. 1, 2, and 3) of brittle graphite/epoxy composites, conducted in the late 1970's, indicated that low-velocity impact resulted in significant reductions in compression-after-impact strength. To improve the compression-after-impact strength of the composite, modifications of existing resins, new rubber-toughened resins, thermoplastics, and interleaving concepts are being developed. Most of these toughened epoxies, advanced thermoplastics, and high-strain fibers have shown only modest improvements in their fracture toughness and damage resistance (refs. 4, 5, and 6). A recent study (ref. 7) showed that two new material systems, IM7/8551-7 and IM6/1808I, have significant improvements in compression-after-impact strengths as compared with brittle graphite/epoxy material systems. However, these materials are expensive and lower cost systems are needed for fabrication of cost-effective aircraft structures. Another approach to improve damage tolerance is to use advanced fiber architectures that provide improved out-of-plane strength. These innovative fiber architectures include "thru-the-thickness" reinforcement such as stitching (ref. 8) and a variety of textile techniques such as weaving, braiding (ref. 9), and knitting (ref. 8).

The objectives of the present investigation were to determine if significant improvements in the interlaminar fracture toughness of a brittle epoxy resin composite could be achieved through the use of woven fabrics and to determine the effect of various weave patterns on the interlaminar fracture toughness. Four woven graphite-fiber fabric styles (plain, oxford, 5-harness satin, and 8-harness satin) were impregnated with Fiberite[1] 934. The mode I critical-strain-energy release rate of the processed laminates was determined using the double cantilever beam (DCB) test. The effects of stacking sequence, specimen thickness, and fabric orientation were investigated. The results from the woven fabric laminates are compared with the results from a 0° unidirectional tape composite.

Materials and Tests

Graphite-Fiber Fabrics

The fabrics tested in this investigation were made from Thornel[2] 300-3K fiber which is a commercially available, continuous high-strength fiber. As shown in figure 1, the fiber was woven into the following fabric styles: plain, oxford, 5-harness satin, and 8-harness satin. For each fabric style the warp yarns are indicated by a dot pattern and the fill yarns are shown in a solid pattern. The following observations are noted for each fabric style. The plain weave fabric has the same yarn pattern for upper and lower surfaces in both the warp and fill directions. The oxford weave fabric has the same yarn pattern for upper and lower surfaces; however, there are differences in the warp and fill directions of each surface. The oxford weave has two fill yarns woven together, whereas the other weave styles have individual warp and fill yarns woven in a repeat pattern. The upper-surface yarn patterns for the harness weave fabrics are dominated by the warp yarn "floats," where a float is a given segment of uncrimped yarn passing over more than one yarn in the orthogonal direction. The lower-surface yarn patterns for the harness weave fabrics are dominated by the fill yarn floats.

The plain weave fabric was woven by Textile Technologies, Inc., and the other three fabrics were woven by the Fiberite Corporation. Each fabric, except the plain weave, had a warp and fill count of 18 ends per inch. The plain weave fabric had a warp and fill count of 19 ends per inch. Also shown in figure 1 is the coordinate system used throughout this investigation.

Epoxy Resin Matrix

All the fabrics were impregnated with Fiberite 934, a 350°F cure thermoset epoxy resin. The resin is based on a tetraglycidyl epoxy (MY720) cured with a diamine curing agent (DDS) (ref. 10). Neat resin mechanical properties can be found in the Fiberite Materials Handbook.

Laminates

The DCB test specimen requires that a simulated crack be machined or fabricated into one end of the

[1] Trademark of the Fiberite Corporation.

[2] Trademark of Union Carbide Corporation.

test specimen prior to testing. In this investigation, strips of 1-mil-thick Kapton[3] or Teflon[3] film were placed at the midplane of the laminates prior to processing to simulate a preexisting crack (ref. 11). The test procedures outlined in reference 11 specify that the warp yarns should be aligned with the longitudinal direction of the DCB specimen. Therefore, a crack-starter strip was placed perpendicular to the warp yarns. Since the effect of fabric orientation on the interlaminar fracture toughness of the various fabrics was desired, crack-starter strips were placed perpendicular to the fill yarns to permit testing in the fill direction of the laminates. The position of the simulated crack with respect to the final dimensions of the test specimen will be detailed in a later section.

The woven fabric was laid up in the following two manners for the oxford, 5-harness satin, and 8-harness satin weave patterns:

1. Two side-by-side stacks of fabric prepreg were laid up to the desired half-thickness. The crack-starter strips were placed in position and the two prepreg stacks were then folded together in a manner similar to that of closing a book. Thus, at the midplane of the laminates, the warp yarn floats of each stack were in contact and parallel to one another. For each fabric an 8-ply and a 16-ply laminate were fabricated using the aforementioned procedure. The material laid up in this manner shall be referred to as being in the "folded" configuration. The folded configuration resulted in symmetric laminates.

2. Two side-by-side stacks of fabric prepreg were laid up to the desired half-thickness and the crack-starter strips were placed in position. One stack was placed directly on top of the other containing the crack-starter strips. Thus, at the midplane the warp yarn floats of one stack were in contact with and perpendicular to the fill yarn floats of the other. This "stacked" configuration resulted in asymmetric laminates. Only 16-ply laminates were fabricated in the stacked configuration.

Differences at the midplane of the two lay-up procedures are illustrated in figures 2 and 3 for the folded and stacked configurations, respectively, for the 8-harness satin weave fabric. Figures 2(a) and 3(a) show a midplane crack growing in the warp direction, and figures 2(b) and 3(b) show the crack growing in the fill direction, respectively, for the folded and stacked configurations.

[3] Trademark of E. I. du Pont de Nemours & Co., Inc.

A very limited supply of the plain weave style of fabric was available. To reduce the amount of material used, a 16-ply laminate was fabricated from 2 plies of plain weave fabric with 7 plies of oxford weave fabric on both the top and bottom. Thus, the laminate was 16 plies thick with a crack-starter strip at the midplane of the laminate between the two plies of the plain weave fabric.

For reasons that will be discussed in a later section, data were desired from a 0° unidirectional T300/934 tape laminate with the fibers normal to the specimen longitudinal axis. A 32-ply T300/934 tape laminate was fabricated with a lay-up of $[0_{15}, 90]_s$. A crack-starter strip was placed between the two 90° plies at the edge of the laminate and aligned with the 90° fabric. This configuration was used to obtain the desired 90° data. Fracture toughness data for a unidirectional $[0]_{24}$ T300/934 tape laminate were available from a previous study (ref. 12) and were used for comparison purposes.

The materials were cured at the NASA Langley Research Center following the manufacturer's recommended cure cycle. The laminates were subsequently C-scanned to detect any voids or anomalies and to verify the correct placement of the Teflon or Kapton crack-starter material. All laminates were acceptable.

Weave Cross Sections

In figures 4 through 7, photographs of polished cross sections of the oxford and 8-harness satin weave laminates are shown in both the warp and the fill directions for the folded and stacked configurations. The folded configuration of the oxford weave is shown in figure 4. In the warp direction, the warp yarn pattern of over two and under two fill yarns is easily discernible. The pattern is regular throughout the thickness with no abrupt change in the pattern at the midplane. In the fill direction of the folded configuration, as shown in figure 4, the relatively straight fill yarns are visible as well as some sizable resin-rich areas.

Polished cross sections of the stacked configuration of the oxford weave in both the warp and the fill directions are shown in figure 5. The pattern of the warp and the fill directions of the stacked configuration looks very similar to the respective patterns of the folded configuration. As previously stated, the top and bottom surfaces of the oxford weave fabric have the same yarn pattern but with differences in the warp and fill directions, and therefore the respective patterns of the folded and stacked configurations are similar, as indicated in figures 4 and 5.

In figure 6 the polished cross sections of the folded 8-harness satin weave in both the warp and the fill directions are shown. The symmetry about the midplane is clearly visible.

In figure 7 the polished cross sections of the stacked 8-harness satin weave configuration in both the warp and the fill directions are shown. In both directions the pattern is similar throughout the thickness and is not disrupted at the midplane. In the stacked configuration, a "top" fabric surface and a "bottom" fabric surface meet at the midplane (see fig. 3), whereas in the folded configuration, two "top" fabric surfaces meet at the midplane. Hence, the stacked configuration is not symmetric about the midplane.

Specimen Geometry and Testing Procedures

A sketch of a double cantilever beam (DCB) specimen is shown in figure 8 along with other pertinent information. The fiber volume fractions were obtained by the acid resin digestion method specified by the American Society for Testing Materials (ASTM D-3171). Specimens were tested in both the warp and the fill directions of the woven laminates. Test specimens in which the warp fibers are parallel to the length of the test specimen shall be referred to as being tested in the warp direction of the fabric, and specimens in which the fill fibers are parallel to the length of the test specimen shall be referred to as being tested in the fill direction of the test specimen.

The DCB specimens of the oxford and satin weaves were 1.5 in. wide and 9 in. long. The crack-starter strips were positioned such that the simulated crack ran the entire width of the specimen and 1.5 in. into the specimen from the outer edge as shown in figure 8.

The plain weave specimens were 1.5 in. wide and 3.5 and 3.25 in. long for the specimens tested in the warp and fill directions, respectively. The crack-starter strips were positioned such that the simulated crack ran the entire width of the specimen and 1.25 in. into the specimen from the outer edge as shown in figure 8.

The $[0_{15}, 90]_s$ tape specimens were 1.5 in. wide and 10 in. long. The tape specimens were tested with the 90° fibers normal to the length of the test specimen. The crack-starter strips were positioned such that the simulated crack ran the entire width of the specimen and 1.5 in. into the specimen from the outer edge as shown in figure 8.

Hinges were bonded as illustrated in figure 8 and, in some cases, were mechanically fastened to the specimens in a manner similar to that outlined in reference 11. Five replicate specimens were fabricated for testing in each test direction, each thickness, and each stacking sequence for the oxford, 5-harness satin, and 8-harness satin weave materials. Four specimens in each test direction of the plain weave material and four specimens of the tape material were fabricated for testing. All specimens were tested; however, occasional bond failures between the hinge and the composite specimen resulted in fewer data obtained than the full number of fabricated test specimens.

The specimens were tested in a screw-driven testing machine. A direct-current displacement transducer (DCDT) was used to measure crosshead motion. A crosshead rate of 0.5 in/min was used. The sides of the specimens were painted with a water-based white paint to aid in crack-length detection. The test procedures and the energy-area integration method of determining the mode I critical-strain-energy release rate (G_{Ic}) outlined in reference 11 were followed.

As previously stated, data from reference 12 for $[0]_{24}$ T300/934 DCB specimens were used for comparison purposes. The 1.0-in. by 10.0-in. specimens were tested in a manner similar to those in the present study except that a crosshead rate of 0.02 in/min was used.

Results

Effect of Thickness

The G_{Ic} values for the 8-ply and 16-ply symmetric (folded) specimens of the oxford, 5-harness satin, and 8-harness satin weaves are shown in figure 9 for the specimens tested in the warp direction and in figure 10 for the specimens tested in the fill direction. Shown above each bar at the top of the figure are the number of data points for which G_{Ic} was calculated for the respective test configuration. The standard deviation is indicated by the range lines drawn through each bar. The results shown in figures 9 and 10 indicate that G_{Ic} was not dependent upon the thickness of the test specimens for either of the three weaves. Since G_{Ic} was not thickness dependent, the remaining laminates were evaluated with 16 plies only.

Effect of Stacking Sequence

Folded configuration. The data shown in figures 9 and 10 indicate significant differences in G_{Ic} as a function of midplane fiber orientations relative to the longitudinal axis of the test specimen. The 16-ply data from figures 9 and 10 are compared in figure 11 along with the 24-ply unidirectional tape data from reference 12. The specimens tested in

the fill direction consistently had a higher G_{Ic} than the specimens tested in the warp direction. The G_{Ic} value of the woven materials was two to eight times greater than that of the 0° unidirectional tape material. Detailed observations of the failure surfaces will be discussed and correlated with test direction in a subsequent section.

Stacked configuration. In figure 12 the warp and fill data in the stacked form are similarly compared with the $[0]_{24}$ tape data from reference 12. For the satin and plain weaves, G_{Ic} was not a function of test direction although the oxford weave still exhibited directional dependency. The large standard deviation obtained for the plain weave fabric could be due to its shorter specimen length which necessitated using much smaller crack-growth intervals. The G_{Ic} values of the woven materials in the stacked configuration were three to six times greater than those of the 0° unidirectional tape material. In the next section detailed observations of the failure surfaces will be discussed and correlated with the stacking sequence.

Failure Surface Observations

Plain weave. As discussed previously, the plain weave specimens were composed of two plies of plain weave fabric at the midplane with seven plies of oxford weave fabric on both the top and bottom. Also recall that the plain weave fabric has the same upper- and lower-surface yarn pattern in both the warp and the fill directions. Figure 13 shows photographs of the failure surface of the plain weave specimens tested in the warp and fill directions; both faces of the failure surface are shown although they are not opposing faces. The failure surfaces of the material tested in both the warp and the fill directions are similar in appearance with respect to fiber breakage and weave pattern. The failure surfaces clearly show that the crack propagated in the plane of the plain weave and did not grow into the oxford weave or the oxford/plain weave interfacial regions.

Oxford weave. Figure 14 shows the failure surfaces of the oxford weave in the folded configuration tested in both the warp and the fill directions. The failure surface of the material tested in the warp direction clearly shows the warp yarns, which are parallel to the direction of crack growth, running over and under the two fill yarns. Since the oxford weave fabric has the same upper- and lower-surface yarn patterns but with differences in the warp and fill directions, both sides of the failure surface of specimens tested in either direction are similar in appearance. However, the failure surfaces of the folded oxford weave specimens were different in appearance depending on the test direction. The failure surfaces of the specimens tested with the warp fibers parallel to the longitudinal axis of the specimen are similar to those of a unidirectional tape material in the sense that little fiber breakage is evident, whereas the failure surfaces of the specimens tested with the fill yarns parallel to the longitudinal axis of the specimen show more fiber breakage.

It is postulated that once a crack has started to grow in the specimens in which the fibers run predominantly parallel to the length of the specimen, the crack grows in the same plane down the length of the specimen. When the crack encounters misaligned fibers, it pulls the fiber out of the matrix and eventually breaks the fiber. In the specimens that have fibers running predominantly across the width of the specimen, the crack either must continually change directions as it grows over or under the fibers or must fracture the fibers. The crack front may not always grow in a straight line across the width of the specimen. It has been shown in DCB specimens made from tape composite materials that the crack front grows in a parabolic shape across the width of the specimen (ref. 13). When the crack front grows in a parabolic manner, the same fiber may be broken in more than one location across the specimen. Therefore, it requires more energy for the crack to continually change directions and to fracture fibers, and this increase in energy results in a higher G_{Ic}.

Figure 15 shows the failure surface of the stacked configuration of the oxford weave. Both sides of the failure surface of the material tested in the warp direction have the same appearance and are similar in appearance to the failure surface of the folded configuration of the oxford weave tested in both the warp direction and the fill direction shown in figure 14.

The similarity between the folded and stacked configurations is not unexpected since the oxford weave pattern is essentially the same when viewed from the top and bottom surfaces (fig. 1). Since the weave pattern is the same on the top and bottom surfaces, the crack growth occurred between plies of the same fabric pattern regardless of the stacking sequence; therefore, the G_{Ic} values would be expected to be approximately the same for both stacking sequences, as, in fact, they were. However, since the warp- and fill-direction yarn patterns were different, the failure surfaces were different and G_{Ic} varied with

the midplane fiber orientation relative to the longitudinal axis of the test specimen.

5-harness satin weave. As shown in figure 1, the pattern of the satin weaves is not the same on the top and bottom surfaces and should result in a failure surface appearance and G_{Ic} dependent on whether two similar or two dissimilar surfaces are located at the crack plane. In figure 16 the failure surfaces of the 5-harness satin weave composite in the folded configuration are shown. Both sides of the failure surfaces are similar. In the warp direction the largest percentage of the visible fibers (warp yarn floats) run parallel to the direction of crack growth, whereas in the fill direction they run perpendicular to the direction of crack growth. The G_{Ic} value was substantially higher for the material tested in the fill direction.

Figure 17 shows the failure surfaces of the stacked configuration of the 5-harness satin weave material. Both sides of the failure surface of the material tested in the warp and fill directions are similar in appearance. The failure surfaces of the stacked configuration generally resemble each other regardless of the test direction, and G_{Ic} is essentially the same for both test directions.

8-harness satin weave. In the folded configuration of the 8-harness satin weave shown in figure 18, both sides of the failure surface for either the warp or the fill test directions are similar in appearance. In the warp direction the largest percentage of visible fibers (warp yarn floats) run parallel to the direction of crack growth, whereas in the fill direction they run perpendicular to the direction of crack growth. In the 5-harness satin weave material in the folded configuration, the specimens with the largest percentage of visible fibers perpendicular to the direction of crack growth had a higher G_{Ic} than those with the largest percentage of fibers parallel to the direction of crack growth.

When the 8-harness satin weave specimens in the stacked configuration are tested in the warp direction (see fig. 19), the floats in the fill direction and the crimped warp yarns are clearly visible in both failure surfaces. Both sides of the failure surface are similar in appearance. The failure surfaces of the stacked 8-harness satin specimens were similar regardless of the test direction, as was the G_{Ic} value for this material in this configuration.

General Findings for Folded Configuration

For all materials fabricated in the folded configuration, G_{Ic} depended on the direction of crack growth. (See fig. 11.) When the largest percentage of the fibers at the midplane were perpendicular to the direction of crack growth, the failure surfaces exhibited more fiber breakage. The additional energy required to break the fibers resulted in a higher G_{Ic} for these materials.

Satin weave specimens tested in the warp direction have fibers predominantly parallel to the direction of crack growth similar to that for a 0° unidirectional tape specimen, whereas satin weave specimens tested in the fill direction have fibers predominantly perpendicular to the direction of crack growth similar to that for a 90° unidirectional tape specimen. More energy was required to propagate the crack when the largest percentage of fibers were perpendicular to the direction of crack growth. Therefore, it was anticipated that a tape laminate tested with fibers 90° to the longitudinal axis would result in a higher G_{Ic}.

Since data from unidirectional tape laminates tested in the 90° direction were not available for comparison, a $[0_{15}, 90]_s$ laminate was fabricated and specimens were machined, as previously described, to evaluate the interlaminar fracture toughness in the 90° direction. Data from these specimens and data from the 0° unidirectional specimens (ref. 12) are shown in figure 20. The G_{Ic} value of the 90° specimens was six times greater than that of the 0° specimens. Figure 21 shows photographs of the failure surface of a $[0_{15}, 90]_s$ specimen. Both sides of the failure surface are similar in appearance. The failure surface shows the 90° plies perpendicular to the direction of crack growth and a portion of the underlying layer of 0° fibers. The crack grew through the 90° plies as well as alternating between the 0° and 90° ply interfaces. The tape data confirm the trend observed for the satin weave and oxford weave data; that is, when the fibers are predominantly perpendicular to the direction of crack growth, the material exhibits a higher interlaminar fracture toughness than when the fibers are predominantly parallel to the direction of crack growth.

Although the G_{Ic} value of the 90° composite was higher than that of the 0° composite, this difference does not translate directly to a higher G_{Ic} for most structural components made from this material system. In general, the direction of maximum loading in structural components is in the same direction as the length of the fibers rather than 90° to the length of the fibers. Typically, structural components are loaded in more than one mode (tension, shear, peel, etc.) which results in a mixed-mode strain-energy release rate controlling the failures due to crack growth.

General Findings for Stacked Configuration

For the materials fabricated in the stacked configuration (see fig. 12), the oxford weave material tested in the fill direction had the highest G_{Ic} and had the majority of fibers running perpendicular to the direction of crack growth. The plain weave material (tested in either the warp or the fill directions) had the next highest G_{Ic}. This material had approximately the same percentage of fibers running both parallel and perpendicular to the direction of crack growth. The oxford weave material tested in the warp direction had the lowest G_{Ic}. Its failure surface was very clean with very few broken fibers.

Concluding Remarks

Results of interlaminar fracture toughness have been obtained from double cantilever beam specimen tests for graphite/epoxy (T300/934) composites for plain, oxford, 5-harness satin, and 8-harness satin weave patterns. The mode I critical-strain-energy release rate (G_{Ic}) was independent of thickness for the 8-ply and 16-ply specimens tested. All the woven fabric materials had a G_{Ic} value significantly higher than that of the 0° unidirectional tape material. Two different stacking sequences (symmetrical and asymmetrical) of the oxford, 5-harness satin, and 8-harness satin weaves were evaluated. The oxford weave exhibited a G_{Ic} that was a function of midplane fabric orientation for both stacking sequences evaluated. The satin weave materials exhibited a G_{Ic} that was a function of fabric orientation but only for the symmetrical (folded) configuration. The directional dependence of G_{Ic} for the fabrics is attributed to the pattern of the yarn "floats" in relation to the direction of crack growth. More energy was required to propagate cracks across the yarns rather than parallel to the yarns, which resulted in a higher G_{Ic}.

In this study, the G_{Ic} value of the fabric-reinforced composites ranged from 0.80 to 3.26 in-lb/in^2, whereas that for the unidirectional composites was 0.5 in-lb/in^2 for approximately equivalent fiber volume fractions. The tape data from the $[0_{15}, 90]_s$ laminate had a G_{Ic} value of approximately 2.4 in-lb/in^2, which confirmed that more energy was required to propagate cracks across the fibers rather than parallel to the fibers. These results clearly demonstrate that woven composites can have a substantially increased G_{Ic} relative to the 0° unidirectional tape composites comprised of the same fiber and matrix materials.

NASA Langley Research Center
Hampton, VA 23665-5225
September 7, 1989

References

1. Rhodes, Marvin D.; Williams, Jerry G.; and Starnes, James H., Jr.: *Effect of Low-Velocity Impact Damage on the Compressive Strength of Graphite-Epoxy Hat-Stiffened Panels.* NASA TN D-8411, 1977.
2. Starnes, James H., Jr.; Rhodes, Marvin D.; and Williams, Jerry G.: *The Effect of Impact Damage and Circular Holes on the Compressive Strength of a Graphite-Epoxy Laminate.* NASA TM-78796, 1978.
3. Byers, Bruce A.: *Behavior of Damaged Graphite/Epoxy Laminates Under Compression Loading.* NASA CR-159293, 1980.
4. Williams, J. G.; and Rhodes, M. D.: Effect of Resin on Impact Damage Tolerance of Graphite/Epoxy Laminates. *Composite Materials: Testing and Design (Sixth Conference)*, I. M. Daniel, ed., Spec. Tech. Publ. 787, American Soc. for Testing and Materials, 1982, pp. 450–480.
5. Williams, Jerry G.: *Effect of Impact Damage and Open Holes on the Compression Strength of Tough Resin/High Strain Fiber Laminates.* NASA TM-85756, 1984.
6. Williams, Jerry G.; O'Brien, T. Kevin; and Chapman, A. J., III: Comparison of Toughened Composite Laminates Using NASA Standard Damage Tolerance Tests. *ACEE Composite Structures Technology—Review of Selected NASA Research on Composite Materials and Structures*, NASA CP-2321, 1984, pp. 51–73.
7. Dow, Marvin B.; and Smith, Donald L.: *Properties of Two Composite Materials Made of Toughened Epoxy Resin and High-Strain Graphite Fiber.* NASA TP-2826, 1988.
8. Dexter, H. Benson; and Funk, Joan G.: Impact Resistance and Interlaminar Fracture Toughness of Through-the-Thickenss Reinforced Graphite/Epoxy. *A Collection of Technical Papers—AIAA/ASME/ASCE/AHS 27th Structures, Structural Dynamics and Materials Conference, Part 1*, 1986, pp. 700–709. (Available as AIAA-86-1020.)
9. Gause, L. W.; and Alper, J. M.: *Mechanical Properties of 'Magnaweave' Composites.* NADC-84030-60, U.S. Navy, Dec. 1983. (Available from DTIC as AD B083 098L.)
10. Fox, Derek J.; Sykes, George F., Jr.; and Herakovich, Carl T.: *Space Environmental Effects on Graphite-Epoxy Compressive Properties and Epoxy Tensile Properties.* NASA TM-89297, 1987.
11. ACEE Composites Project Office, compiler: *Standard Tests for Toughened Resin Composites—Revised Edition.* NASA RP-1092, 1983. (Supersedes NASA RP-1092, 1982.)
12. Funk, Joan G.; and Sykes, George F.: The Effects of Radiation on the Interlaminar Fracture Toughness of a Graphite/Epoxy Composite. *J. Compos. Technol. & Res.*, vol. 8, no. 3, Fall 1986, pp. 92–97.
13. Davidson, B. D.; and Schapery, R. A.: Effect of Finite Width on Deflection and Energy Release Rate on an Orthotropic Double Cantilever Specimen. *J. Compos. Mater.*, vol. 22, no. 7, July 1988, pp. 640–656.

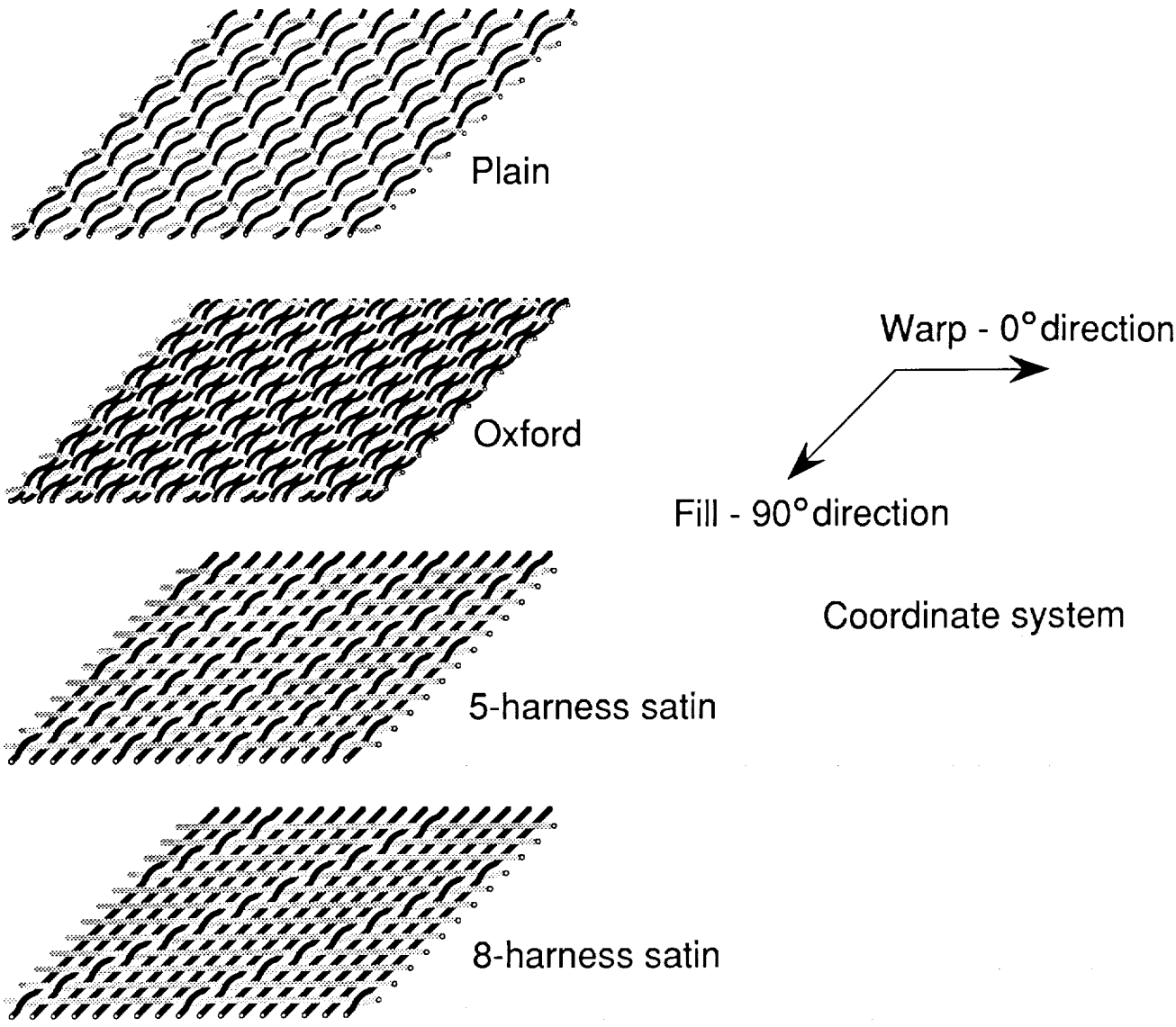

Figure 1. Yarn patterns of plain, oxford, 5-harness satin, and 8-harness satin weaves.

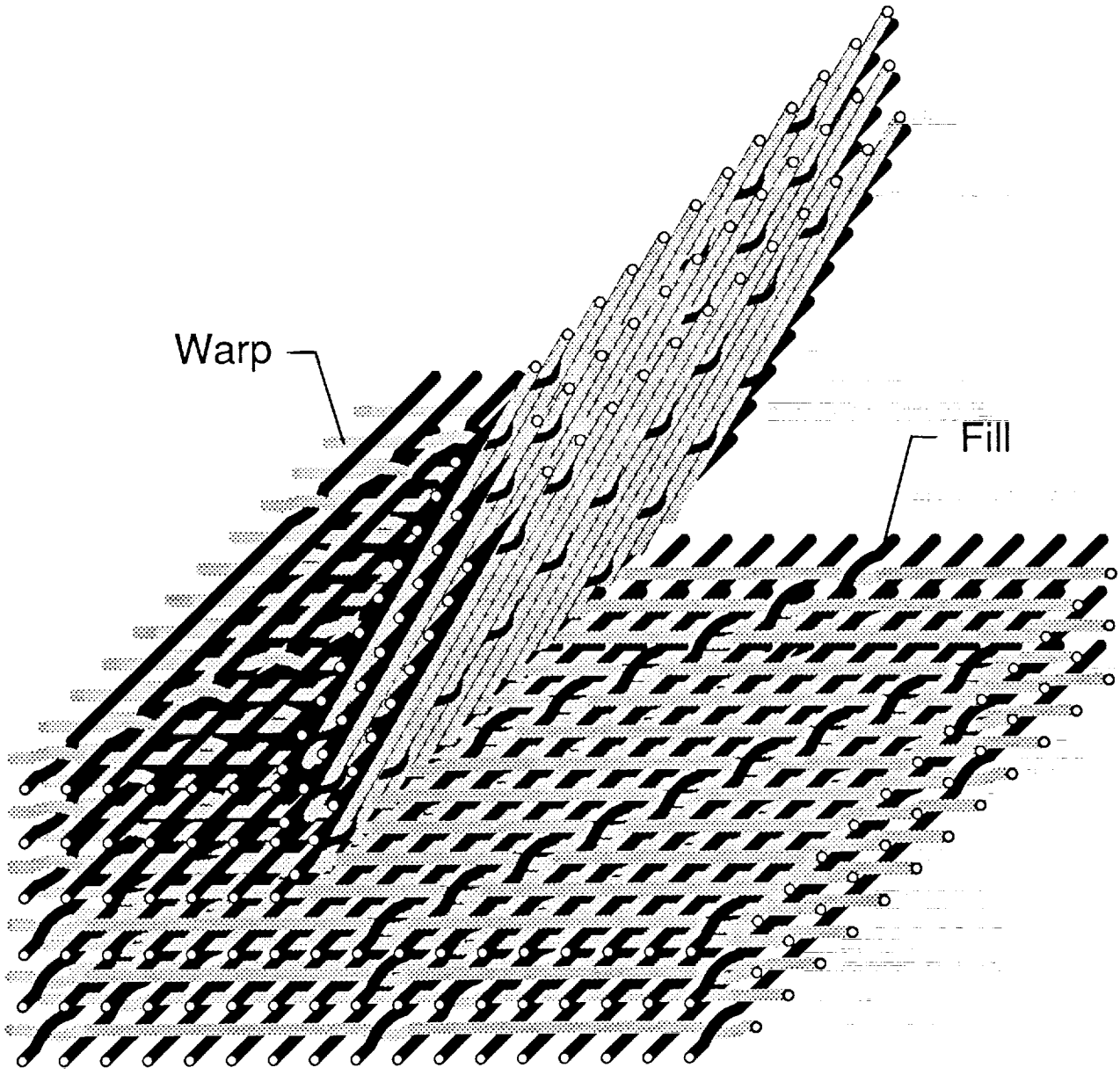

(a) Midplane crack growing in warp direction.

Figure 2. 8-harness satin weave fabric in the folded configuration.

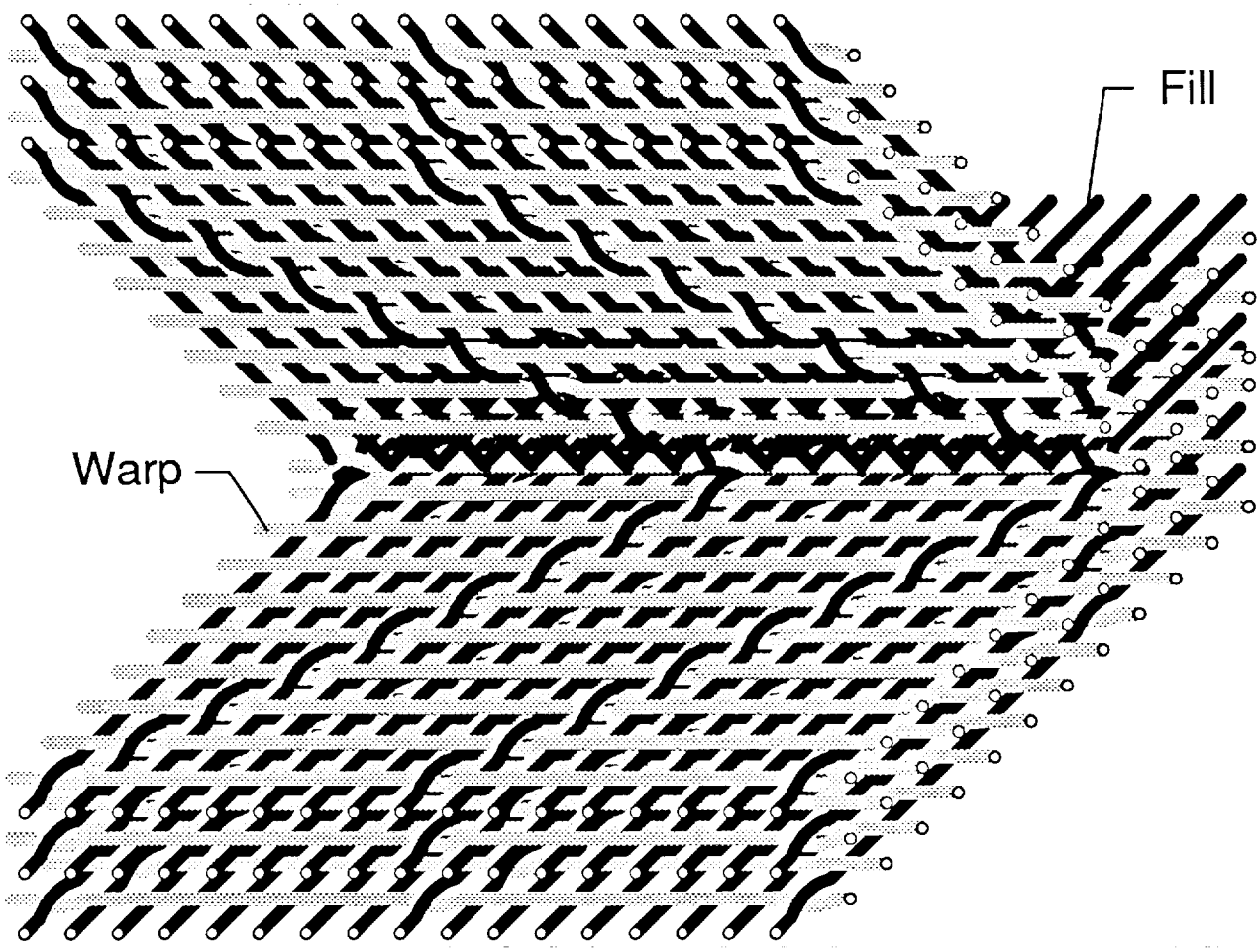

(b) Midplane crack growing in fill direction.

Figure 2. Concluded.

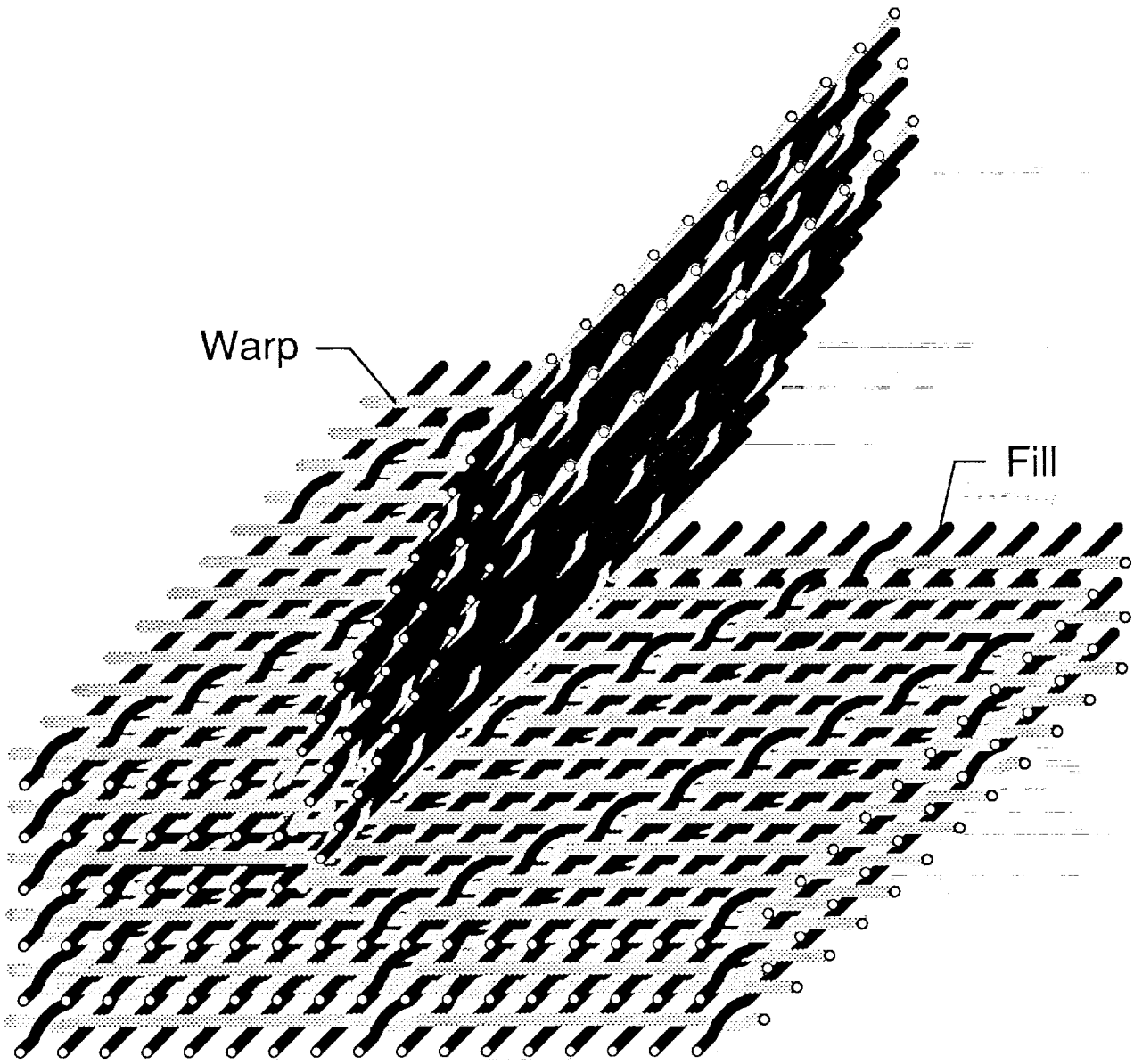

(a) Midplane crack growing in warp direction.

Figure 3. 8-harness satin weave fabric in the stacked configuration.

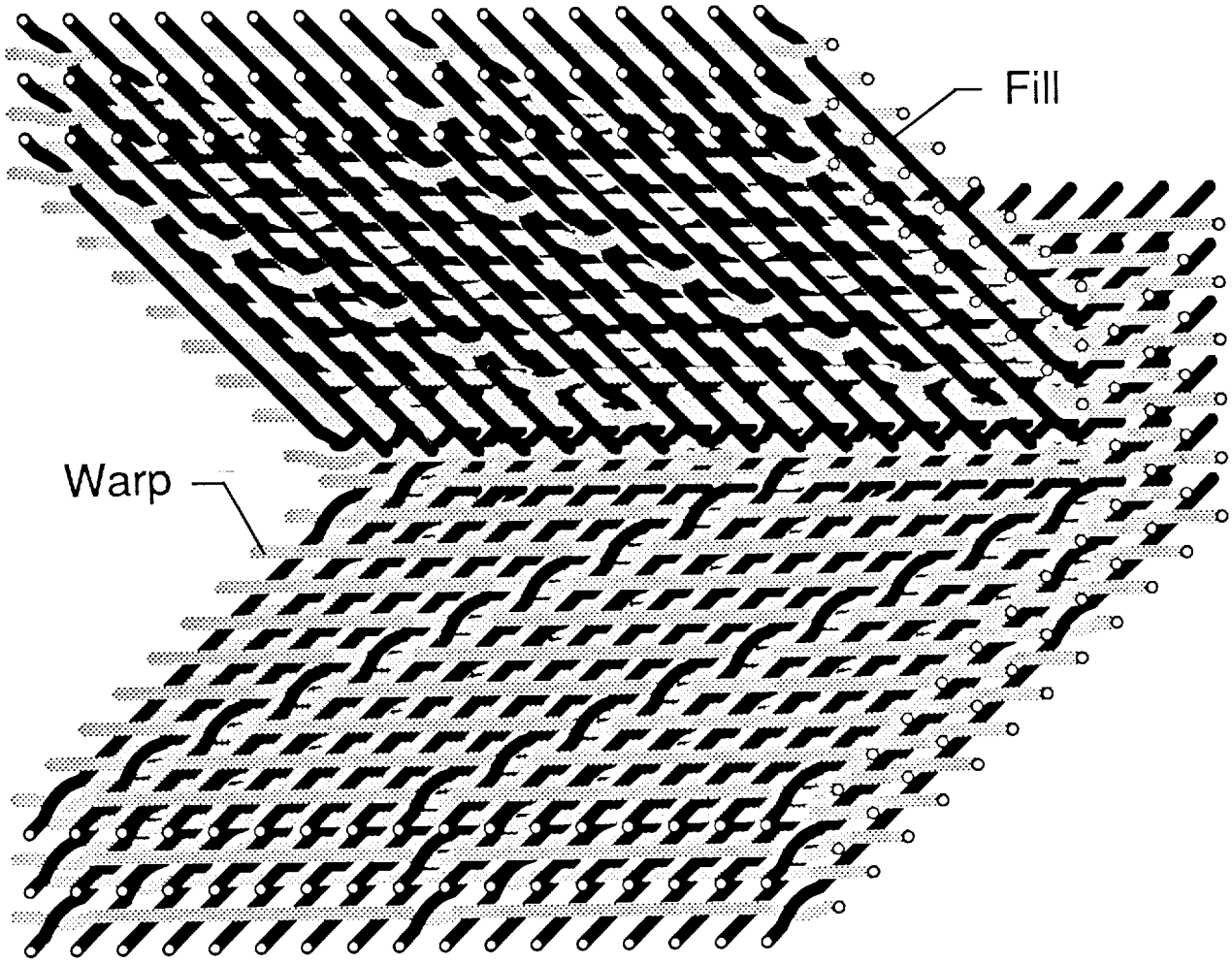

(b) Midplane crack growing in fill direction.

Figure 3. Concluded.

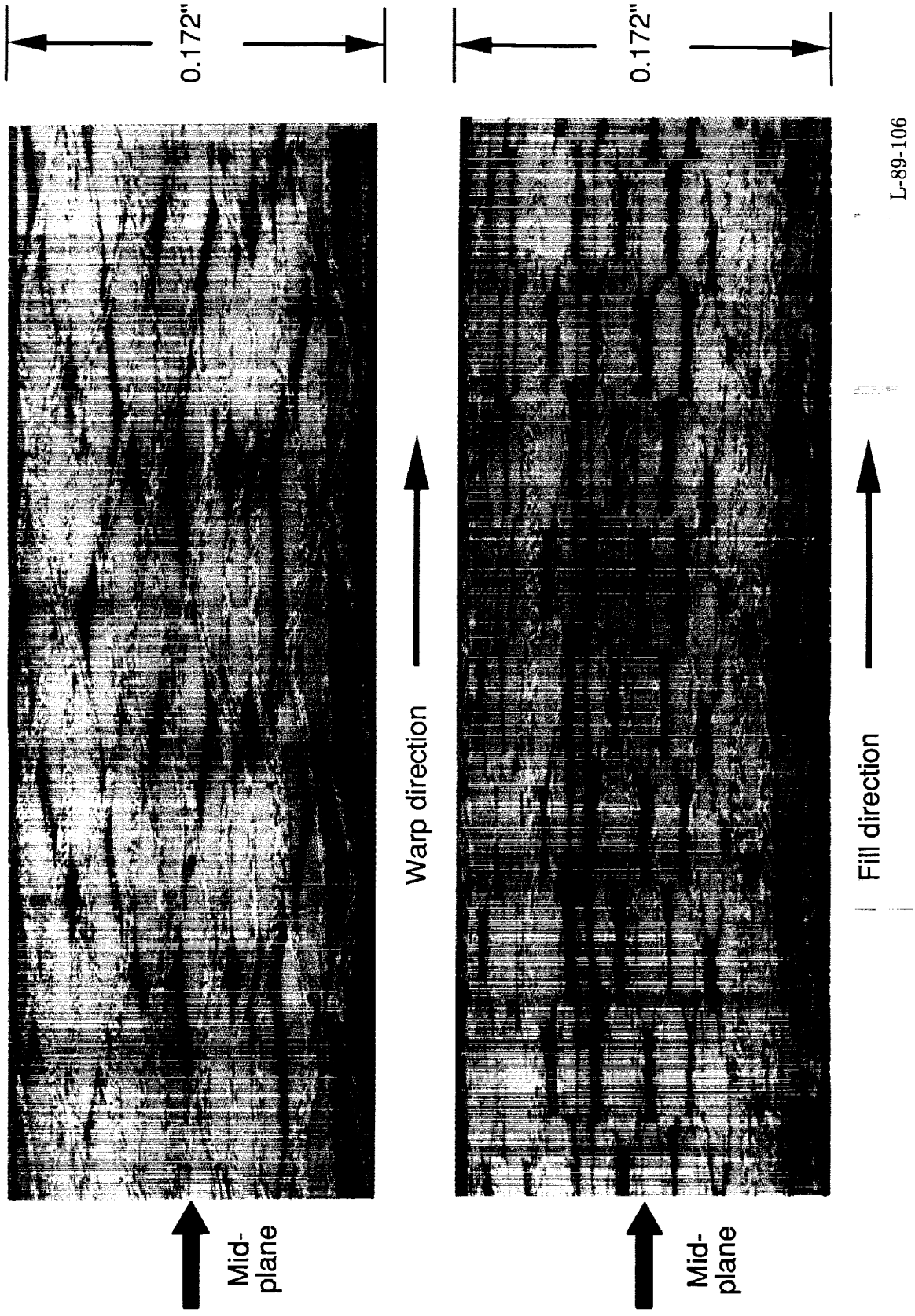

Figure 4. Polished cross sections of the folded configuration of an oxford weave laminate.

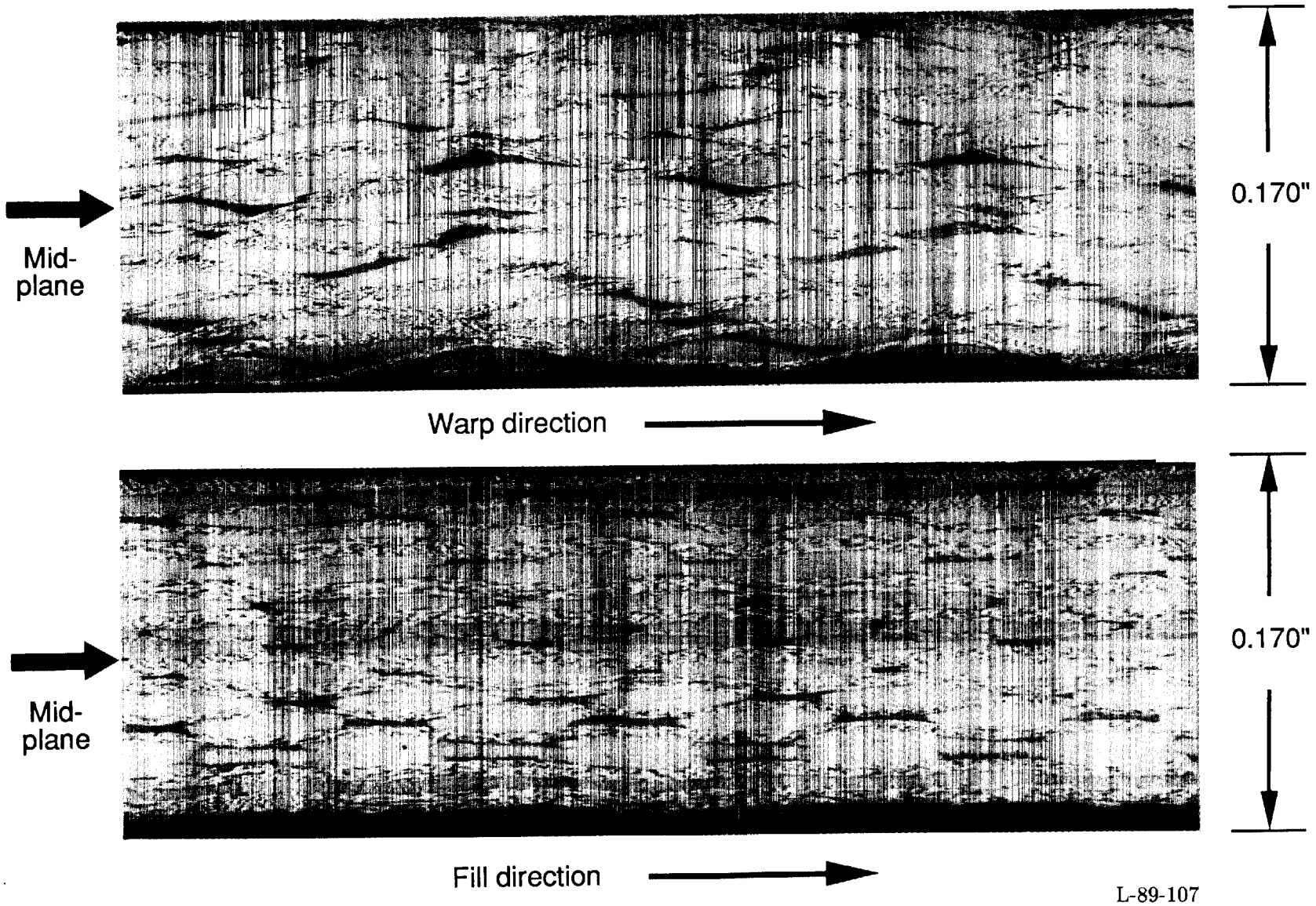

Figure 5. Polished cross sections of the stacked configuration of an oxford weave laminate.

L-89-108

Figure 6. Polished cross sections of the folded configuration of an 8-harness satin weave laminate.

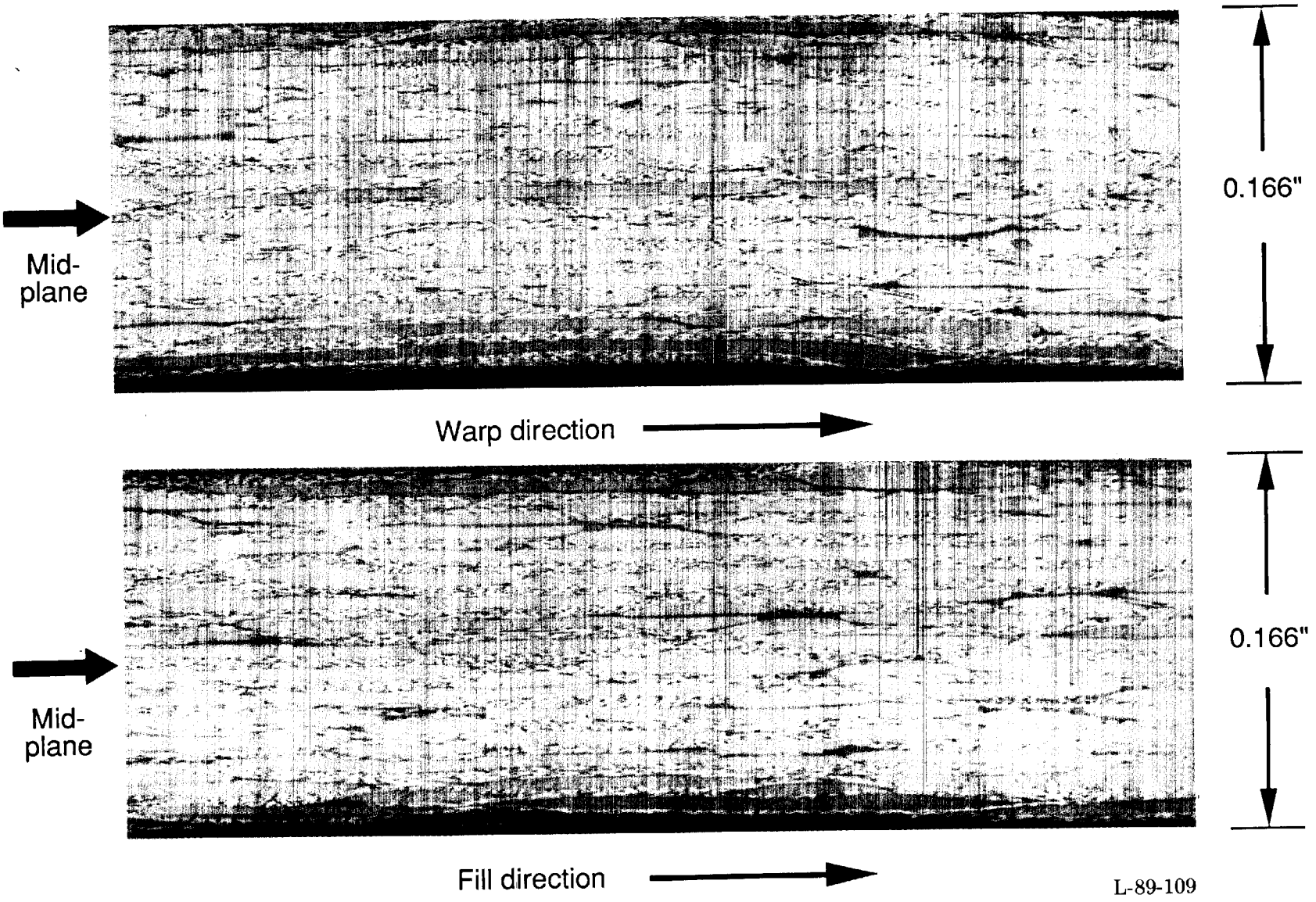

Figure 7. Polished cross sections of the stacked configuration of an 8-harness satin weave laminate.

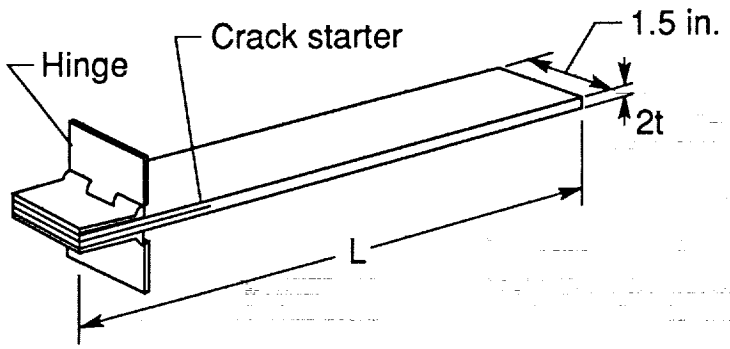

Weave pattern	Ply orientation (a)	Lay-up procedure	2t, in.	L, in.	Fiber volume fraction, percent
Oxford	$[0]_{4s}$	Folded	0.087	9.0	64.5
	$[0]_{8s}$	Folded	.172	9.0	59.4
	$[0]_{16}$	Stacked	.170	9.0	59.2
5-harness satin	$[0]_{4s}$	Folded	0.086	9.0	64.2
	$[0]_{8s}$	Folded	.170	9.0	63.7
	$[0]_{16}$	Stacked	.169	9.0	61.6
8-harness satin	$[0]_{4s}$	Folded	0.089	9.0	64.6
	$[0]_{8s}$	Folded	.164	9.0	63.0
	$[0]_{16}$	Stacked	.166	9.0	62.2
Plain [b]	$[0]_{16}$	Stacked	0.162	{3.50 (warp) 3.25 (fill)}	66.6
Tape	$[0_{15}, 90]_s$	(c)	.153	10.0	65.9

[a] 0° direction corresponds to warp direction of fabric.

[b] $[\text{Oxford}_7, \text{Plain}]_s$.

[c] Not applicable.

Figure 8. Double cantilever beam specimen and test parameters.

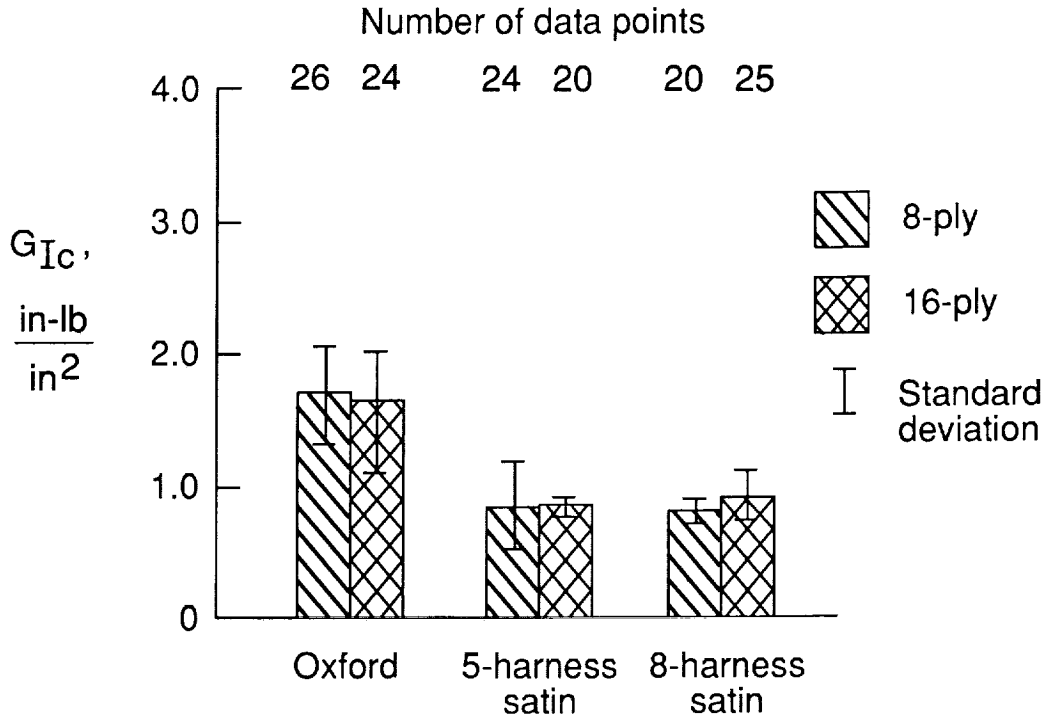

Figure 9. Values of G_{Ic} of the 8-ply and 16-ply folded-configuration laminates tested in the warp direction.

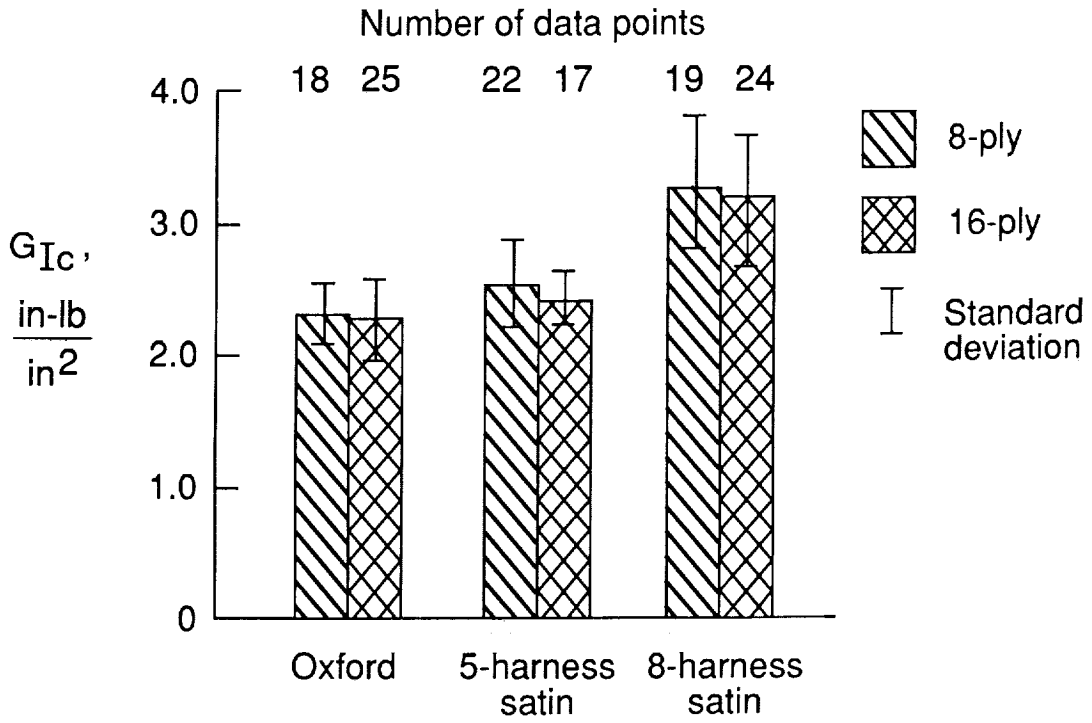

Figure 10. Values of G_{Ic} of the 8-ply and 16-ply folded-configuration laminates tested in the fill direction.

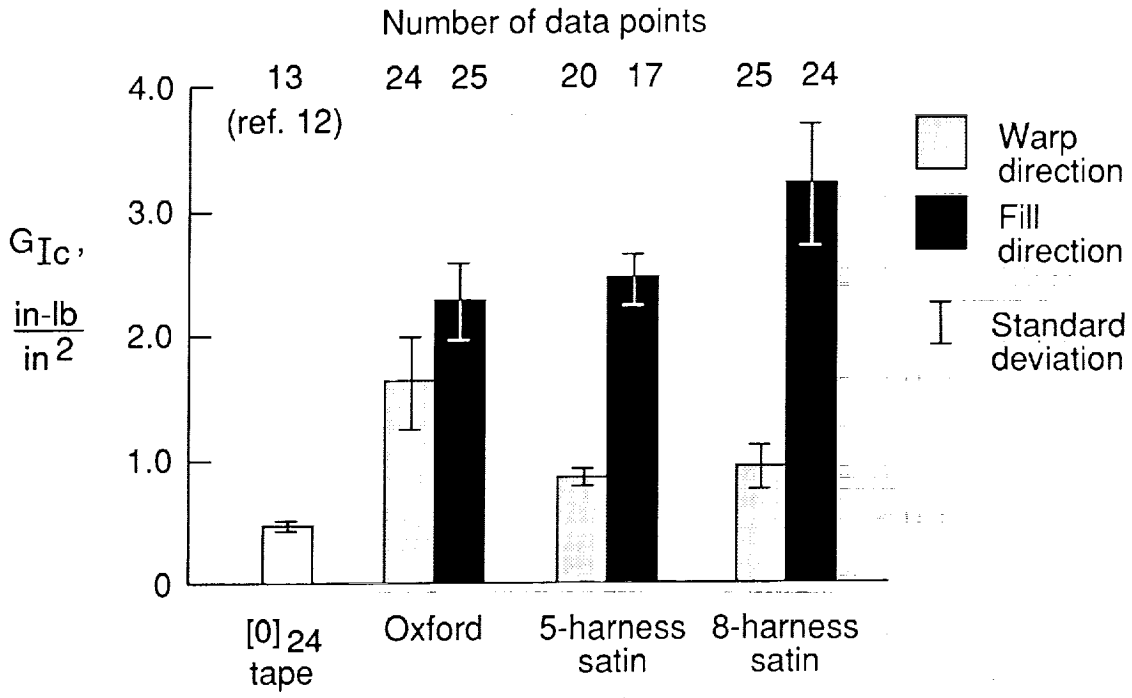

Figure 11. Values of G_{Ic} of the folded-configuration laminates in both the warp and the fill directions.

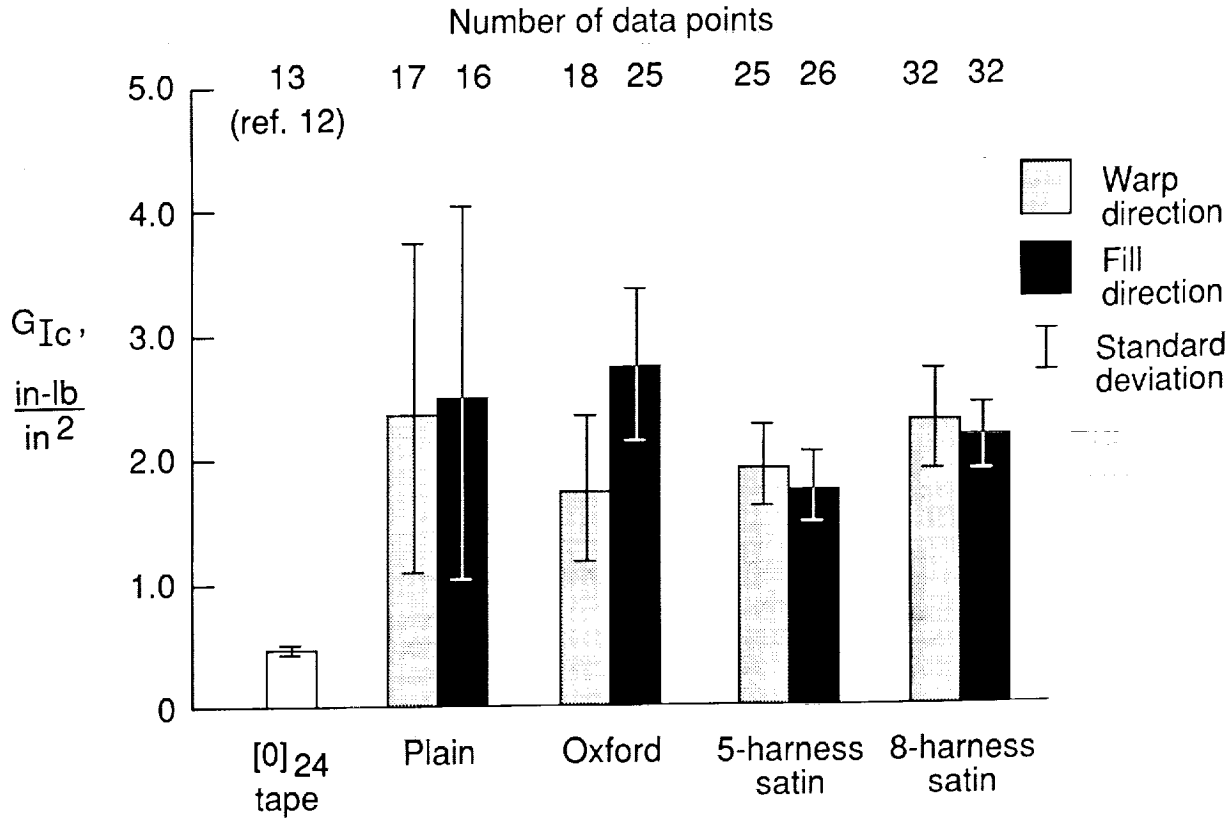

Figure 12. Values of G_{Ic} of the stacked-configuration laminates in both the warp and the fill directions.

ORIGINAL PAGE
BLACK AND WHITE PHOTOGRAPH

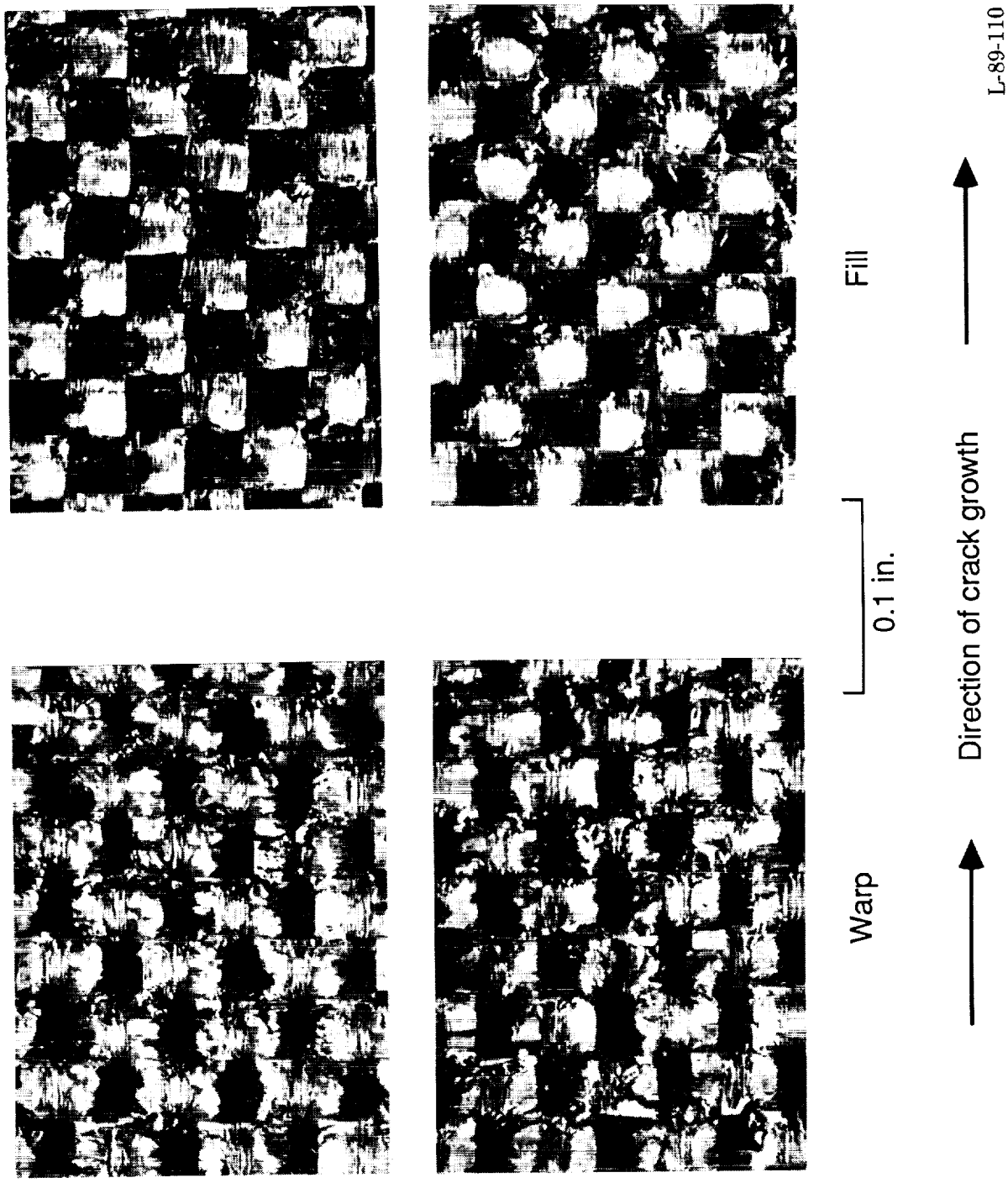

Figure 13. Failure surfaces of plain weave specimens in the stacked configuration.

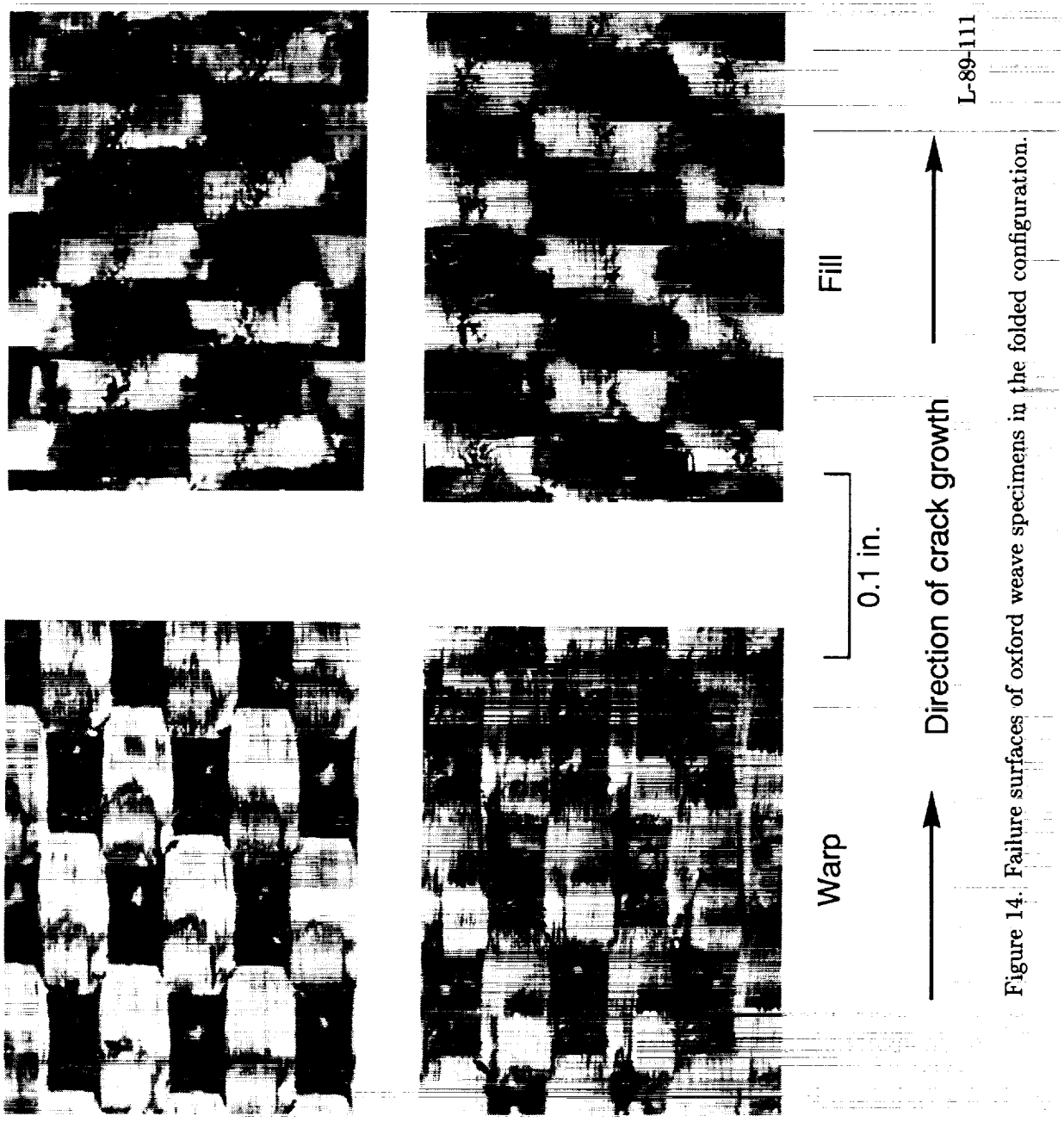

Figure 14. Failure surfaces of oxford weave specimens in the folded configuration.

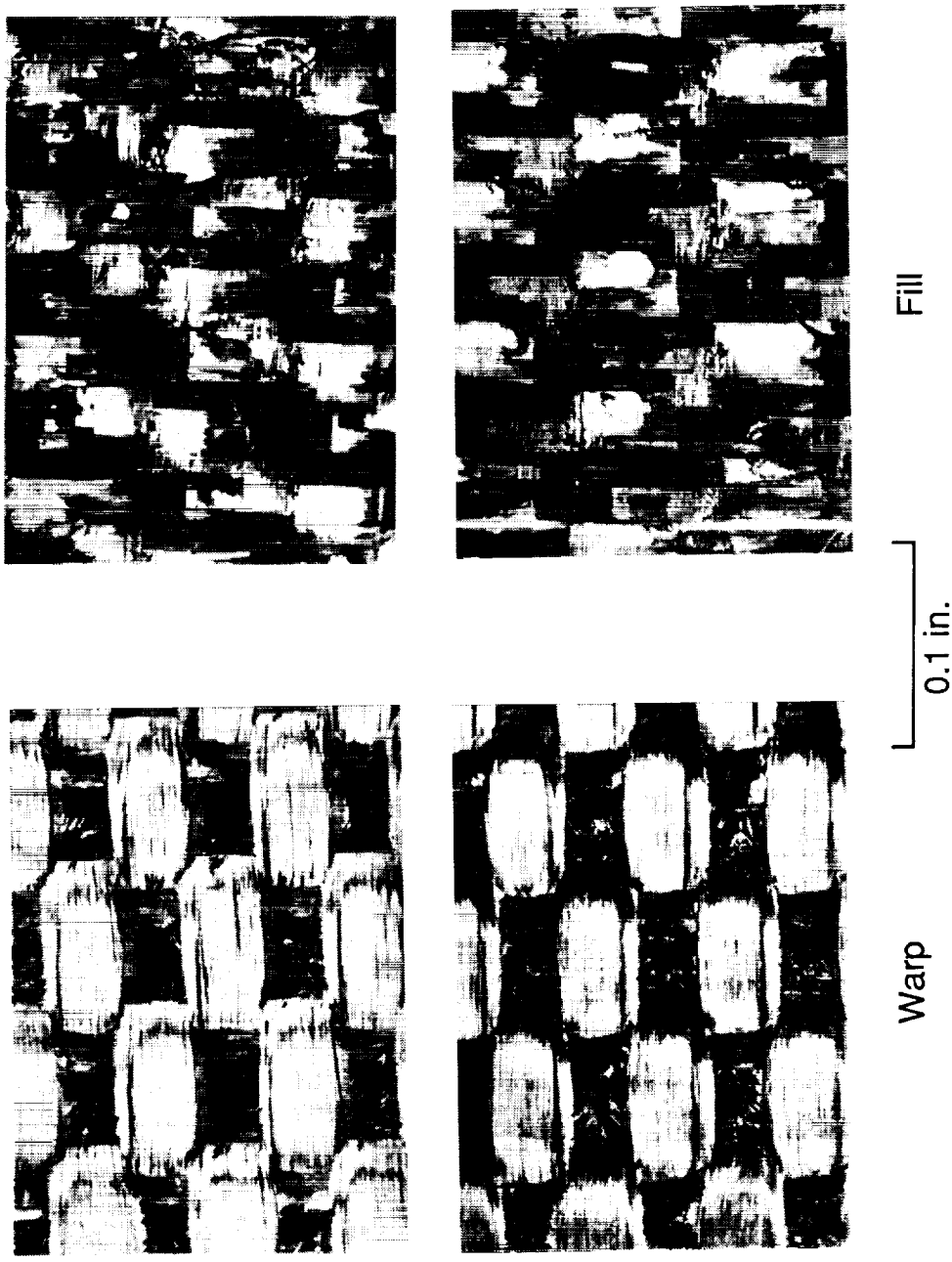

Figure 15. Failure surfaces of oxford weave specimens in the stacked configuration.

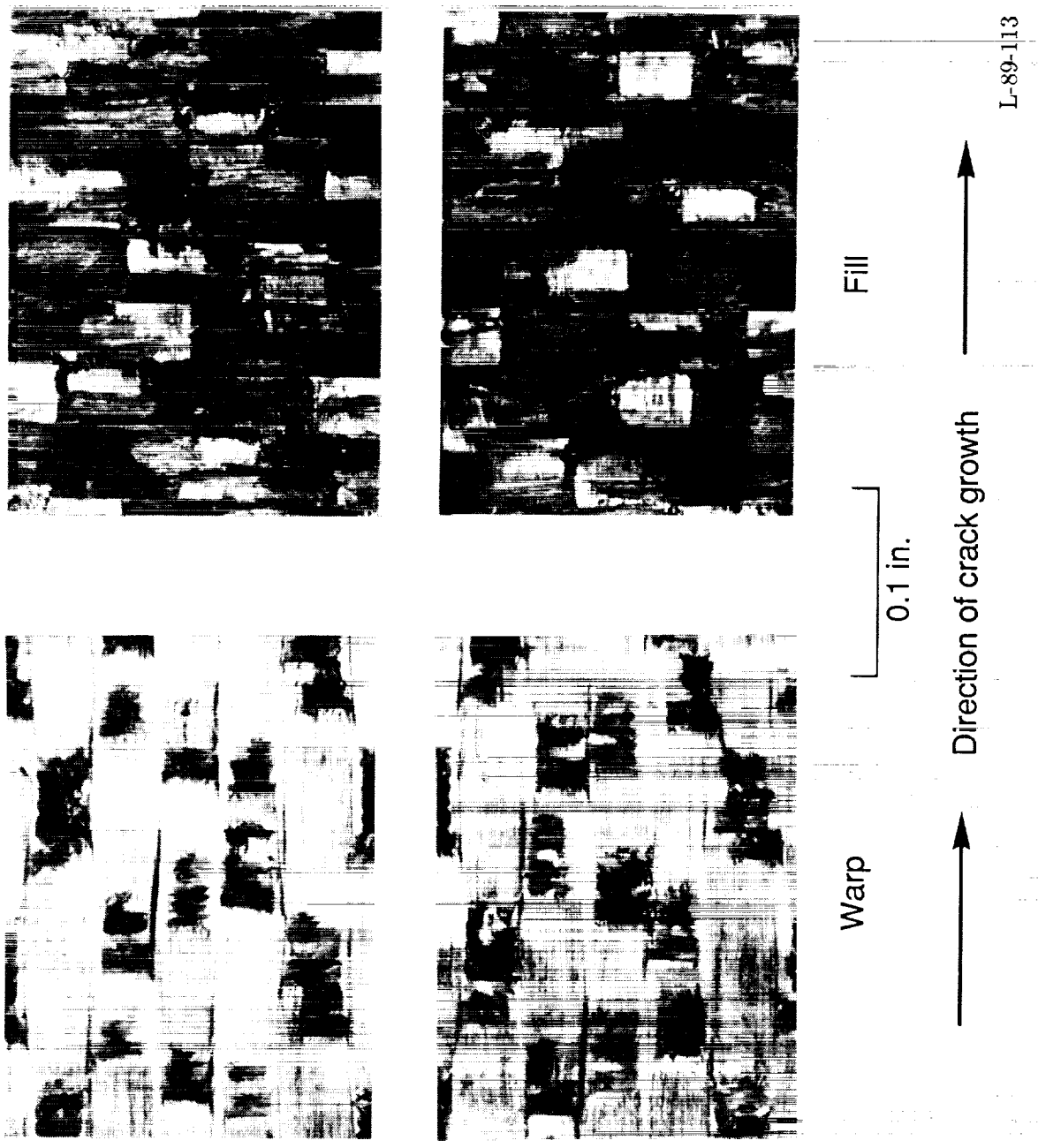

Figure 16. Failure surfaces of 5-harness satin weave specimens in the folded configuration.

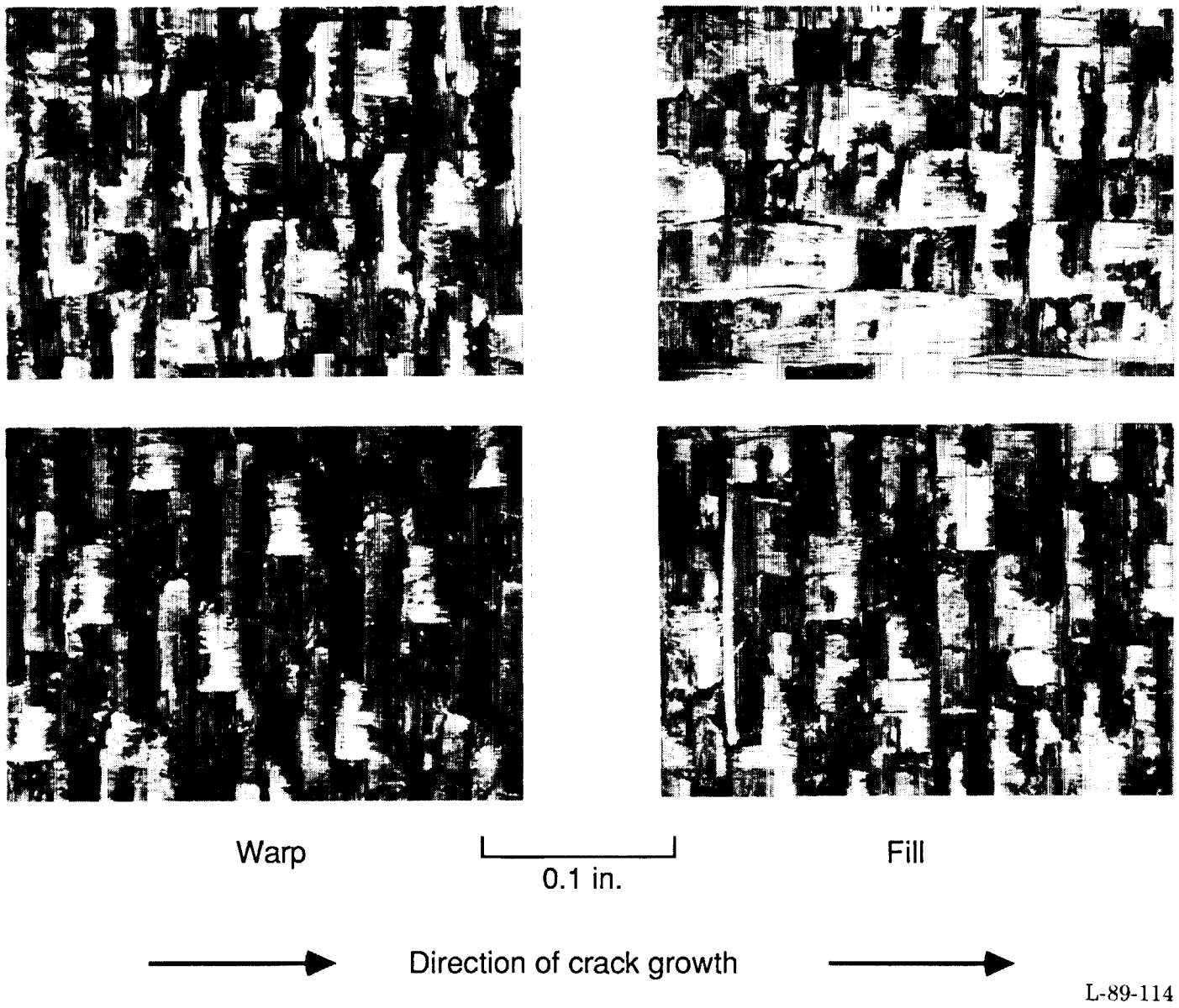

Figure 17. Failure surfaces of 5-harness satin weave specimens in the stacked configuration.

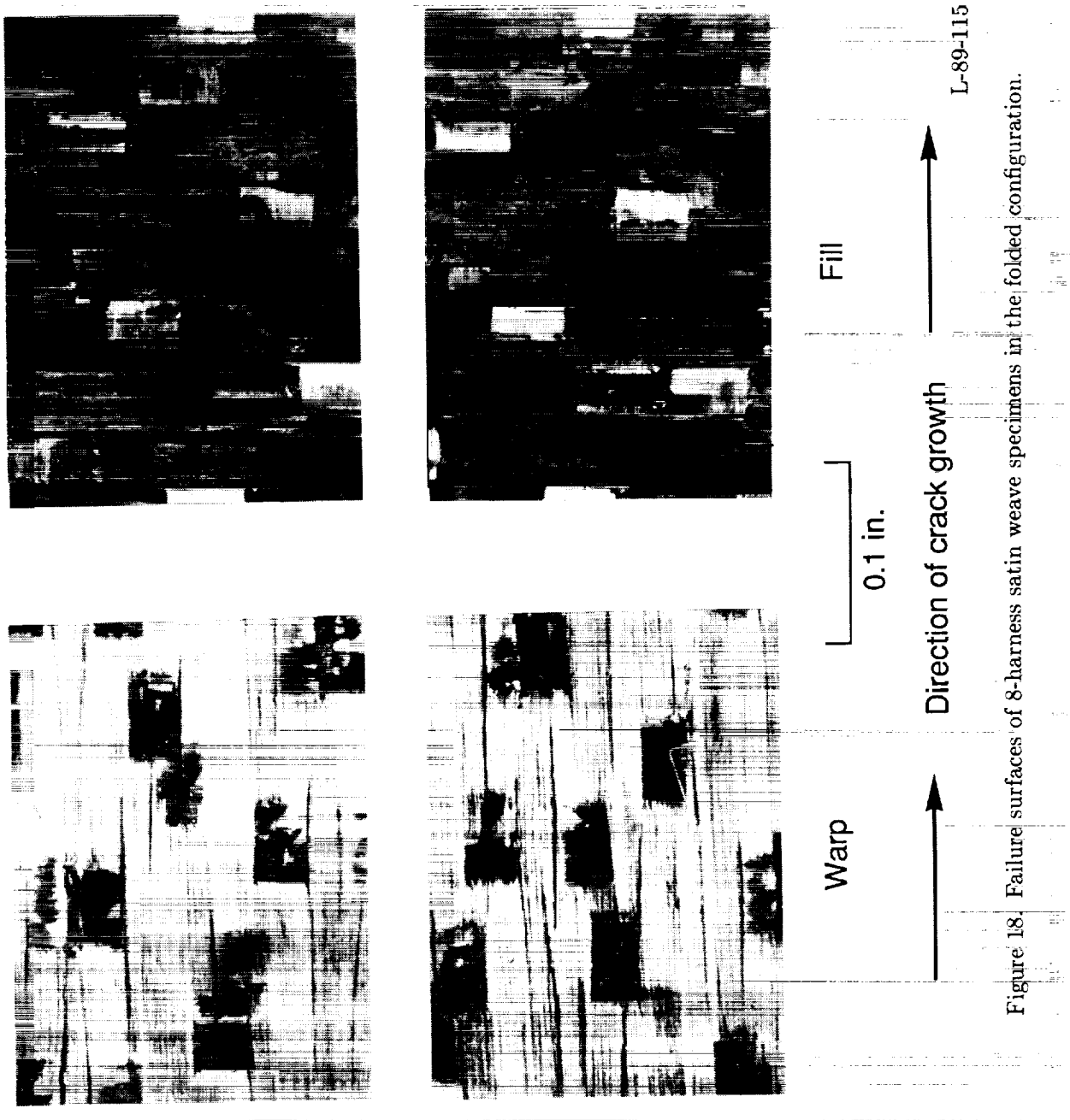

Figure 18. Failure surfaces of 8-harness satin weave specimens in the folded configuration.

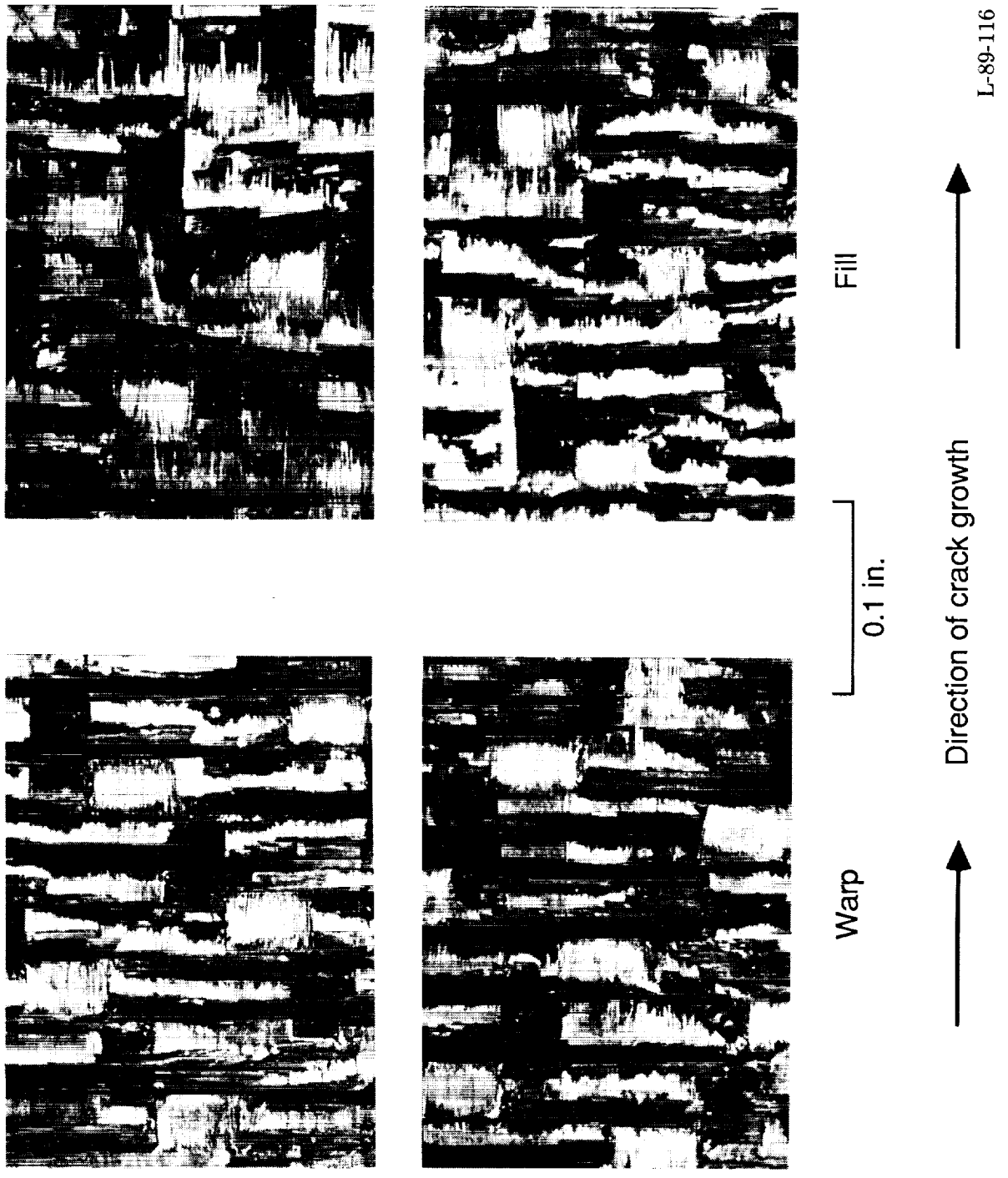

Figure 19. Failure surfaces of 8-harness satin weave specimens in the stacked configuration.

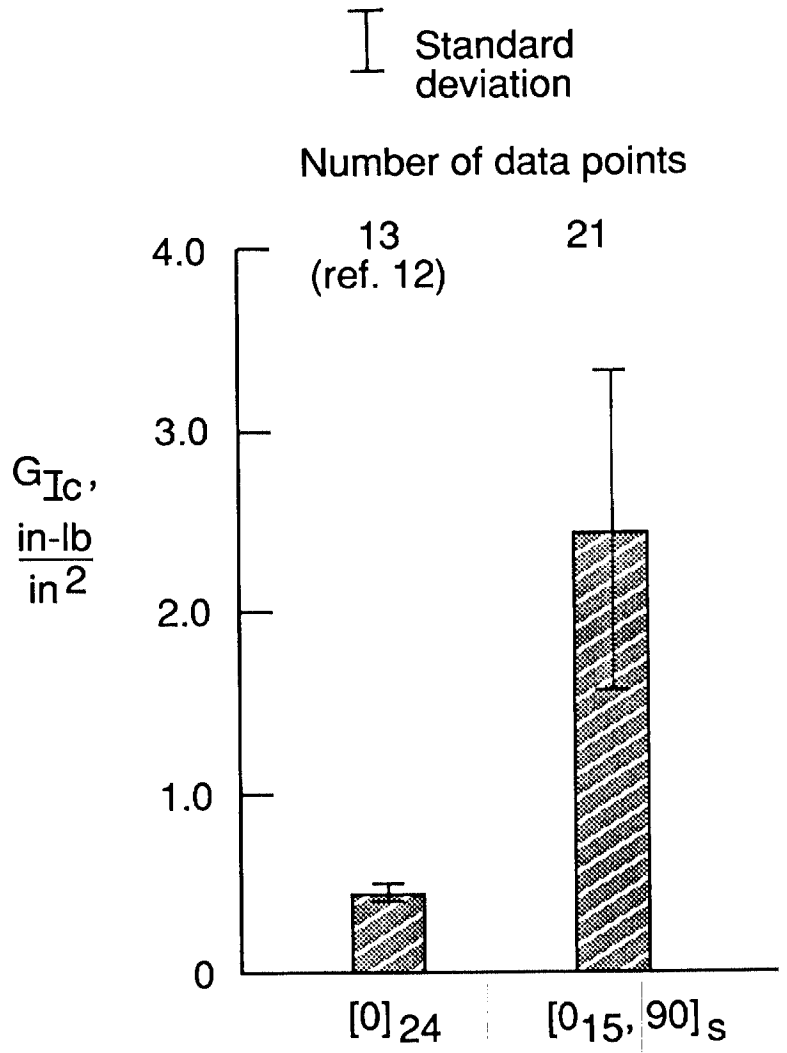

Figure 20. Effect of fiber orientation at midplane of tape specimens on measured value of G_{Ic}.

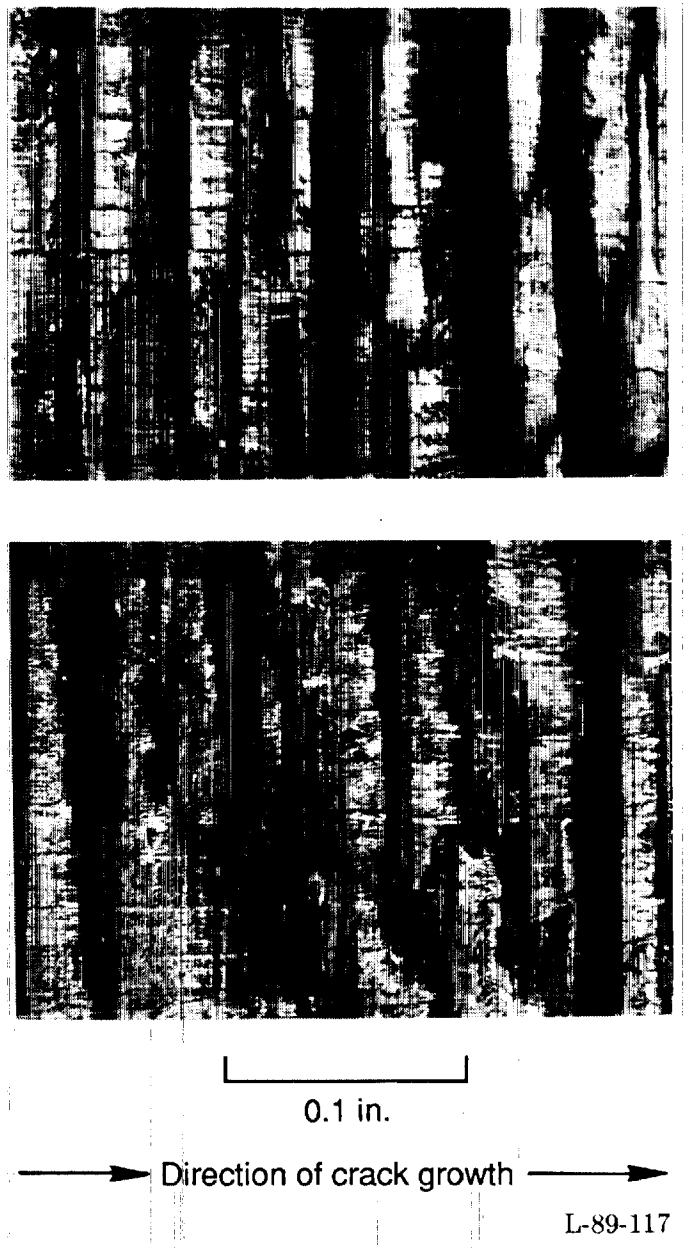

Figure 21. Failure surfaces of $[0_{15}, 90]_s$ specimen.

NASA
National Aeronautics and Space Administration

Report Documentation Page

1. Report No.	2. Government Accession No.	3. Recipient's Catalog No.
NASA TP-2950		

4. Title and Subtitle	5. Report Date
The Interlaminar Fracture Toughness of Woven Graphite/Epoxy Composites	November 1989
	6. Performing Organization Code
7. Author(s)	8. Performing Organization Report No.
Joan G. Funk and Jerry W. Deaton	L-16629
9. Performing Organization Name and Address	10. Work Unit No.
NASA Langley Research Center Hampton, VA 23665-5225	505-63-01-06
	11. Contract or Grant No.
12. Sponsoring Agency Name and Address	13. Type of Report and Period Covered
National Aeronautics and Space Administration Washington, DC 20546-0001	Technical Paper
	14. Sponsoring Agency Code

15. Supplementary Notes

16. Abstract

The interlaminar fracture toughness of graphite/epoxy woven composites was determined as a function of stacking sequence, thickness, and weave pattern. Plain, oxford, 5-harness satin, and 8-harness satin weave patterns of a T300/934 fabric were evaluated by the double cantilever beam test. The fabric had a mode I critical-strain-energy release rate (G_{Ic}) ranging from two to eight times greater than that of a 0° unidirectional T300/934 tape material. The interlaminar fracture toughness of a particular weave pattern was dependent on whether the stacking sequence was symmetric or asymmetric and, in some cases, on the fabric orientation.

17. Key Words (Suggested by Authors(s))	18. Distribution Statement
Woven fabric Composites Interlaminar fracture toughness Mode I critical-strain-energy release rate	Unclassified—Unlimited Subject Category 24

19. Security Classif. (of this report)	20. Security Classif. (of this page)	21. No. of Pages	22. Price
Unclassified	Unclassified	27	A03

NASA-Langley, 1989

For sale by the National Technical Information Service, Springfield, Virginia 22161-2171